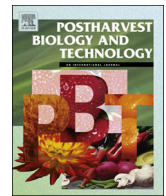




ELSEVIER

Contents lists available at ScienceDirect

Postharvest Biology and Technology

journal homepage: www.elsevier.com/locate/postharvbio

Selection of an optimized metal oxide semiconductor sensor (MOS) array for freshness characterization of strawberry in polymer packages using response surface method (RSM)

Mahdi Ghasemi-Varnamkhasti^{a,b,*}, Ayat Mohammad-Razdari^{a,*}, Seyedeh Hoda Yoosefian^a, Zahra Izadi^{a,b}, Gholamreza Rabiei^c

^a Department of Mechanical Engineering of Biosystems, Shahrekord University, 8818634141, Shahrekord, Iran

^b Nanotechnology Research Center, Shahrekord University, 8818634141, Shahrekord, Iran

^c Department of Horticultural Science, Shahrekord University, 8818634141, Shahrekord, Iran

ARTICLE INFO

Keywords:

Electronic nose
Strawberry
Response surface
Optimized sensors

ABSTRACT

An eight metal oxide semiconductor sensor (MOS) based electronic nose (e-nose) has been used to characterize freshness of strawberry in different polymer package types. Pattern recognition methods such as principal component analysis (PCA), linear discriminant analysis (LDA), and support vector machine (SVM) were used to classify and investigate the effects of polymer packages on strawberry freshness. The packages were Ethylene Vinyl Alcohol (EVOH), Polypropylene (PPP), and Polyvinyl chloride (PVC). The response surface method (RSM) was considered for selection of optimized sensor array in terms of the contribution of each sensor in sample classification. Sample headspace patterns were examined on days 1, 8 and 16. The results revealed that PCA explains 84% of the variance between the data. The LDA classified samples with an accuracy of 86.4%. The SVM method with polynomial function could accurately recognize samples as C-SVM by 86.4% and 50.6% in training and validation, and as Nu-SVM by 85.2% and 55.6% in training and validation with a radial basis function, respectively. Finally, among the eight sensors used in the study, MQ8, MQ3, TGS813, MQ4, and MQ136 sensors were selected as optimal response sensors using RSM to reduce the cost of fabrication. Furthermore, optimal application sensors for each polymer package were identified using RSM.

1. Introduction

One of the most practical and non-destructive ways to investigate the quality of food is the electronic nose (e-nose) system. This system simulates the sense of human olfactory and detects the headspace of the samples with an array of sensors (Ghasemi-Varnamkhasti et al., 2011, 2015). It is a high-performance and precise method which provides enough information and specifications of food in the form of data in a fast and reliable way. E-nose consists of two stages of diagnosis and analysis, and these two stages include signal detection, extraction of features, and data output with specific patterns. It also provides effective and useful information for development of regression models demonstrating the food quality attributes (Men et al., 2018).

Optimization includes studying the optimum conditions of the problems, creating a suitable model and determining the algorithm for solving, creating the theory of convergence for algorithms and numerical experiments with common problems and the problems that

occur in real conditions (Gadhiya et al., 2018). The theory and methods of optimization, which are relatively new methods in mathematics, analytical mathematics, and research problems, are used in engineering domains, business management, military industry and space technology. RSM as an optimization approach consists of a set of solutions which are used to examine optimal operating conditions through experimental methods. This method includes performing various tests using the results of an experiment to guide a route to be followed later (Moradi et al., 2018).

Food packing films have a uniform and integrated structure with a thickness of less than 0.01 in. (Emamifar et al., 2011). There exist some reported studies in the literature dealing with the packaging films for postharvest quality examination. Ghasemi-Varnamkhasti et al. (2018a) conducted a study on the properties of polymer packages of polyethylene on fungi. According to the results, this type of package maintained the product freshness and also delayed the corruption and its physical and chemical changes.

* Corresponding authors.

E-mail addresses: ghasemymahdi@gmail.com (M. Ghasemi-Varnamkhasti), am.razdari@gmail.com (A. Mohammad-Razdari).

So far, various studies have been conducted in the field of e-nose systems to investigate the authenticity of foodstuffs, such as milk (Tohidi et al., 2018), sunflower oil (Haddi et al., 2013), cumin (Tahri et al., 2017), saffron (Kiani et al., 2017), olive oil (Jolayemi et al., 2017; Ordukaya and Karlik, 2017), and shallow rice (Baskar et al., 2017).

According to previous reports and to the best of our knowledge, this study is the first research conducted on the use of RSM combined with chemometrics approaches for selection of an optimized gas sensors array to characterize the strawberry freshness in polymer packages. Packaging strawberries in well-ventilated warehouses under controlled conditions to increase the freshness is costly and needs high energy. On the other hand, the mass production of this fruit in Iran leads researchers toward using precise engineering techniques to improve the quality of the fruit. Therefore, polymer package was used as an effective way to preserve strawberry fruit quality. At the following, the head space of packages was investigated by e-nose, and the best optimized sensor in the e-nose system was selected using RSM.

2. Materials and methods

2.1. Sample preparation

Fresh strawberries (*Fragaria Ananasa cv. 'Gaviota'*) were harvested at full size (length 4 cm and diameter 3 cm fruit size average) with more than 75% red color. Fruit were stored in small sterile plastic containers (20 × 15 × 6 cm) and transported to the laboratory after harvest.

To pack samples, Polyvinyl chloride (PVC) (with a thickness of 2 mm, permeable against moisture and O₂), Polypropylene (PPP) (with a thickness of 0.5 mm, impermeable against moisture and gases) and Ethylene Vinyl Alcohol (EVOH) (with a thickness of 3 mm, resistant to oxygen penetration) were prepared from the Iranian Polymer Research Institute. When the fruit were cleaned with hand and transferred to the laboratory environment, all samples were placed at 18 °C for 1 h, to reach balance with the environment. A 15 strawberries were randomly selected and placed in the cylindrical package (with height of 20 and diameter of 10 cm). Packages were sealed and three replicates (three packed cylinder) were considered for each treatment. The packages were then placed in a refrigerator at 4 °C and 75% relative humidity (Silva et al., 2016) and data was then taken on days 1, 8 and 16.

2.2. The structure of the e-nose system

An e-nose consisting of eight gas sensors was designed and developed in our laboratory to determine the freshness of the strawberries in polymer packages. The system included oxygen capsules, sensor chamber, sampling chamber, data acquisition card, and air flow valves (Fig. 1). Eight sensors such as TGS2602, TGS2620, TGS813 and TGS822 were purchased from Figaro Engineering, Inc. (Glenview, USA), three sensors containing MQ3, MQ8 and MQ136 were provided from HANWEI Electronics Co. (Hanwei, China) and one obtained from FIS (Osaka, Japan) that were engaged in a Teflon cylindrical chamber

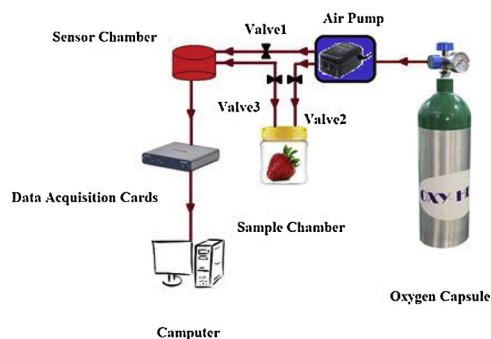


Fig. 1. Schematic representation of electronic nose system.

Table 1

Specification and application of sensors used in sensor array.

Sensors	Detection ranges (ppm)	Gas Target
TGS813	500-10000	Methane, Ethanol, Propane, Isobutene, Hydrogen
MQ8	100-10000	Hydrogen (H ₂)
MQ4	200-10000	Methane, natural gas
TGS822	50-5000	Organic solvent vapor
MQ136	1-200	Hydrogen Sulfide H ₂ S (gas)
MQ135	10-300	Alcohol, Ammonia-benzene-carbon dioxide (CO ₂)
MQ-3	0.05-10	Alcohol
FIS	1-10	Air quality control - hydrogen sulfide

which worked at constant temperature. The most prominent features of this type of sensor are its long life, high response to moisture, high chemical resistance and low price. Each of these sensors reacts to certain combinations of volatile substances in the chamber (Table 1). For more details on the instrumentation system, the reader can refer to Ghasemi-Varnamkhasti et al. (2018b).

The operation stages of the e-nose system include baseline correction, measurement, and purging of the sensor chamber. The baseline correction step was performed to provide a steady state for the sensor array response. At this stage, the carrier gas (oxygen) was injected into the sensor chamber through the pump for 170 s (valve 1 was open and valves 2 and 3 were closed). These sensors require oxygen to function. Any change in the volatile material gas leads to the oxidation reactions at the sensor surface, which in turn results in a change in the sensor resistance (Moon et al., 2018). At the measurement stage, the oxygen gas enters into the sample chamber and transfers the sample headspace to the sensor chamber. A duration of 230 s maximized the sensor response (valve 1 was closed and valves 2 and 3 were open). The purging step was performed to reach the sensor responses to the baseline and prepare the system for subsequent experiments. The carrier gas was injected into the sensor chamber for 110 s (valve 1 was open and valves 2 and 3 were closed).

2.3. Pre-processing and preparing data extracted from sensor signal

The purpose of pre-processing data is to detect sensor responses and to increase the accuracy in analyzing detection patterns. The pre-processing stage includes baseline correction, compression, and normalization. Baseline correction is performed to improve the quality of the sensors response using three methods, including differential, fractional and relative function (Kiani et al., 2018). The average of the last 10 data at the measurement step was used to perform the pattern recognition methods. In this research, the fractional method was used to correct the baseline. The fractional method has been widely used in MOS sensors to correct the baseline (Eq. (1)) and normalize the data (Sanaeifar et al., 2016).

$$y_r(t) = \frac{x_r(t) - x_r(0)}{x_r(0)} \quad (1)$$

In the Eq. (1), $x_r(t)$ is the sensor response at time t , $x_r(0)$ is the lowest sensor response before the measurement step and $y_r(t)$ is the pre-processed response. The next step is to compare responses with the aim of constructing a feature vector for all sensors. For this purpose, the highest sensor response at the headspace injection step is considered as the feature. In the last step, data were normalized for each sensor (s) in the range within 0–1 using Eq. (2).

$$y_r^s = \frac{x_r^s - \min_{v_k}[x_r^s]}{\max_{v_s}[x_r^s] - \min_{v_s}[x_r^s]} \quad (2)$$

In the Eq. (2), x_r^s represents the sensor response, $\min_{v_k}[x_r^s]$ is the lowest response and $\max_{v_s}[x_r^s]$ is the highest response in the measurement phase (Sanaeifar et al., 2016).

2.4. Data analysis

2.4.1. Principal component analysis (PCA)

The PCA method is a statistical method that uses orthogonal transmission to transform a set of observed correlated variables into a set of non-correlated linear variables that are the main components. This transformation is such that the first major component has a high variance and then the other components also have high variances, with limits that interact with the previous components (Ait-Sahalia and Xiu, 2018). PCA is a sensitive and high-precise method for finding principal variables, and it is one of the most common ways for data analysis and dimension reduction in multivariate systems (Esteki et al., 2017). Also, data loading diagrams of the sensor set in PCA are provided (Ghasemi-Varnamkhasti et al., 2015). The pattern recognition was used to investigate the distinction between different polymer packages on d 1, 8 and 16 of storage.

2.4.2. Linear discriminant analysis (LDA)

The linear discriminant analysis method creates a linear combination of all the features that make the classification in a series of samples. This function increases between-group variance and reduces within-group variance. Transformation and transmission in this function are performed in such a way that with the entrance of new observations, the maximum quantity is obtained to predict the between groups variance (Tharwat et al., 2017; Varmuza and Filzmoser, 2009).

2.4.3. Support vector machine (SVM)

The SVM method was introduced by Wapnik et al. (1998). The purpose of this method is to find an optimal plate with the smallest distance between all data and points. The SVM training algorithm assigns a new model to the data set or transforms the data into non-probable boundary linear classification (Zhou et al., 2015). The result of this model is a representation of data in a multidimensional space, where data have been categorized in classes and are characterized by a separating hyperplane between data. The new data are also in the same space and their classification is based on the range that is placed on the plate. In other words, given labeled training data (supervised learning), the algorithm outputs an optimal hyperplane which categorizes new examples (Fig.2) (Esteki et al., 2017).

All PCA, LDA and SVM analyses were performed using Unscrambler x10.4 software (CAMO AS, Trondheim, Norway).

2.4.4. Determination of optimal conditions using RSM

The effect of two independent variables (storage time and package type) on dependent variable (sensor response) was studied using Historical Data Design. This method can be used for the variables that are incapable of being tested and also do not have central factors (Karami et al., 2016). It is assumed that there are two mathematical functions f_k for y_k which are as follows.

$$y_k = f_k(\varepsilon_1, \varepsilon_2) \tag{3}$$

where, $(\varepsilon_1, \varepsilon_2)$ are the natural variables in natural unit, ε_1 represents the

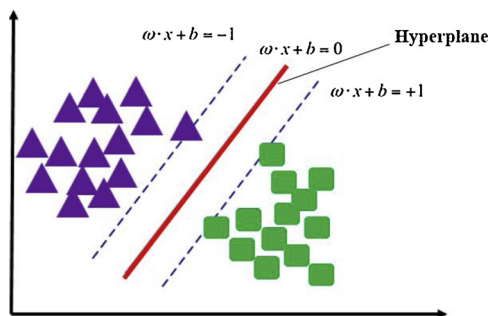


Fig. 2. Schematic of SVM classification method.

Table 2 Independent test variables and selective levels in process analysis.

Levels		Natural variables		Coded variables		Independent variables
1 (-1)	8 (0)	16 (+1)	ε_1	X1		Time (Day)
Control (+1)	EVOH (+2)	PPP (+3)	PVC (+4)	ε_2	X2	Package

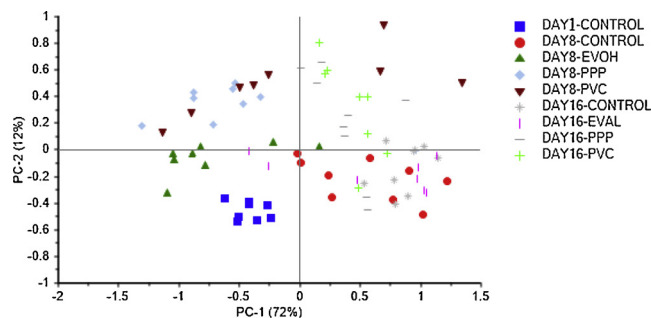


Fig. 3. Score plot of PCA analysis for strawberry polymer packages on the days 1, 8 and 16 of storage.

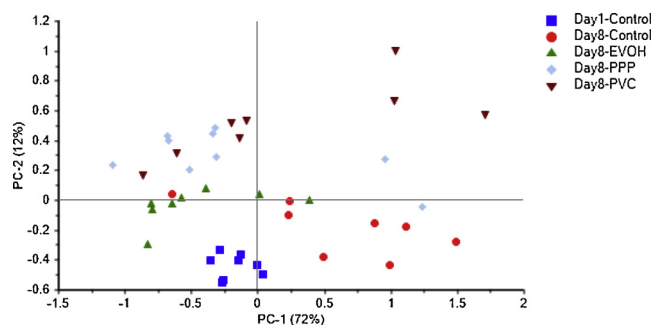


Fig. 4. Score plot of PCA analysis for strawberry polymer packages on days 1, 8 and 16 of storage.

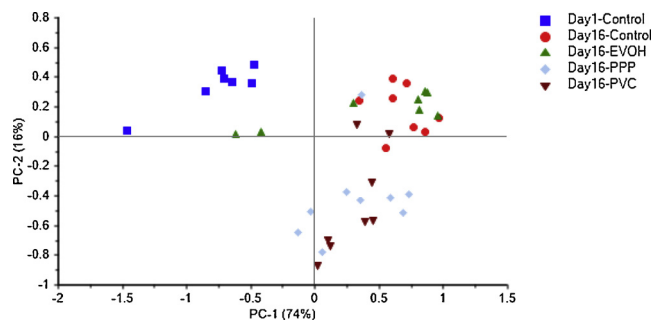


Fig. 5. Scores plot of PCA analysis for strawberry polymer packages on days 1, 8 and 16 of storage.

storage time entered and ε_2 is the type of polymer package. In response surface problems, natural variables are converted to the encoded variables (x_1, x_2) .

$$y_k = f_k(x_1, x_2) \tag{4}$$

In this research, a second-order polynomial model (Lin et al., 2007) was used to model the process.

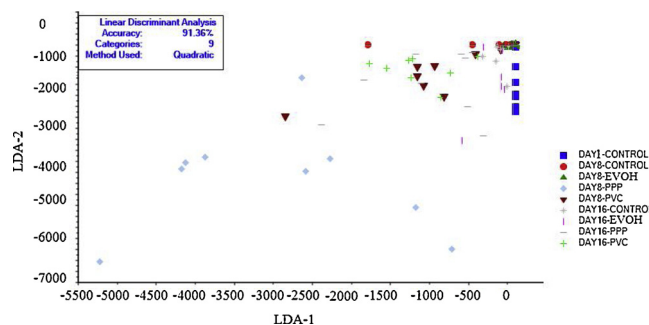


Fig. 6. LDA analysis for strawberry polymer packages on the days 1, 8 and 16 of storage.

Table 3
Results and comparison of Nu-SVM and C-SVM models subjected to the kernel functions.

Kernel function	C-SVM				Nu-SVM			
	c	γ	Train	Validation	Nu	γ	Train	Validation
Linear	4.64	–	64.19	50.61	0.44	1	71.60	51.85
Polynomial	0.21	4.64	86.41	50.61	0.44	1.66	75.30	48.14
Radial Basis Function	0.21	1.66	56.79	51.85	0.33	0.59	85.18	55.55
Sigmoid	0.21	0.07	44.44	43.20	0.55	0.07	61.72	53.08

$$y_k = \beta_0 + \sum_{i=1}^2 \beta_i x_i + \sum_{i=1}^2 \beta_{ii} x_i^2 + \sum_{i=1}^2 \sum_{j=i+1}^2 \beta_{ij} x_i x_j \quad (5)$$

In Eq. (5), y_k is the predicted response considered as dependent variables ($k = 1, 2, \dots, 8$). X_i is the encoded input variable or the independent variable ($i = 1, 2$). The value of the independent variables was encoded between -1 and +1 and the package type was encoded from +1 to +4. β is the regression coefficients parameter. Using the second-order model, five mathematical models were evaluated for each dependent variable in the mentioned form. In this plan, 45 testing units were obtained at a central point to determine the error value (Table 2).

The experimental design, process optimization and ANOVA on second order model coefficients were developed using Design Expert 10 software. Significant terms in the model were obtained by using variance analysis for each response.

3. Results and discussion

3.1. PCA

According to PCA results, there is a significant difference between the control and polymer packages strawberry samples. PC1 and PC2 explained 72% and 12% of the variance among the samples,

respectively (Fig. 3), and overall, 84% of the total variance of the data was explained. Based on the results, control samples were completely separated by PCA. On day 8 of storage, the EVOH package was also significantly distinguished from control, PPP, and PVC packages. This result means that strawberry samples in EVOH packages did not change much during storage, which depends on the structure of the EVOH package. Because EVOH prevents the entry of oxygen into the package and does not allow the respiration of the fruit. On the day 8 of storage (Fig. 4), the two components of PC1 and PC2 explained 72% and 12% of the variance among the samples, respectively, and accounted for 84% of the total variance of data. At this storage time, all samples in the polymer package are distinguished from control and PPP while PVC packages are not well differentiated, but the EVOH package is completely distinguished from other packages. On the day 16 of storage (Fig. 5), PC1 and PC2 could explain 74% and 16% of the variance among samples, respectively, and overall, accounted for 90% of the total variance of data. At this time, in addition to the complete differentiation of packages from the control samples, the EVOH package can be distinguished from PPP and PVC packages, and the packages have been classified separately. In a study conducted by Liu and Tang (2017) using the artificial nose and PCA method, the headspace of the samples was accurately categorized by 92%. Qiu et al. (2015) also classified strawberries using e-nose and electronic tongue (e-tongue) with PCA method with an accuracy of 99.8%. Pan et al. (2014) also predicted strawberry fungal diseases using e-nose and PCA pattern recognition. Qiu et al. (2014) categorized strawberry juice using e-nose coupled with PCA method.

3.2. LDA

The score diagram according to the first two main components (LD1-LD2) is shown in Fig. 6. The LDA method was used to evaluate the potential of headspace recognition system. According to the results, this method had a high capability (with an accuracy of 91.4%) for classification of the odor patterns of polymer and control packages on the days 1, 8 and 16. According to the results, on the days 1, 8 and 16 of storage, the control and all polymer packages of EVOH, PPP, and PVC have been well distinguished. Qiu et al. (2015) classified strawberries using e-nose and e-tongue using the LDA method with an accuracy of 99.9%. Qiu et al. (2014) also classified strawberry juice using the e-nose and LDA with a very high precision.

3.3. SVM

Two types of C-SVM and Nu-SVM were used to classify samples in the SVM method. The parameters Nu, C and γ were validated using trial and error by minimization. Four types of kernel functions including linear, polynomial, radial base and sigmoid were also used. In the C-SVM method, the polynomial function had the highest accuracy in the classification of strawberry samples in the polymer package with an accuracy of 86.41% for training and 50.61% for validation. Also, in the

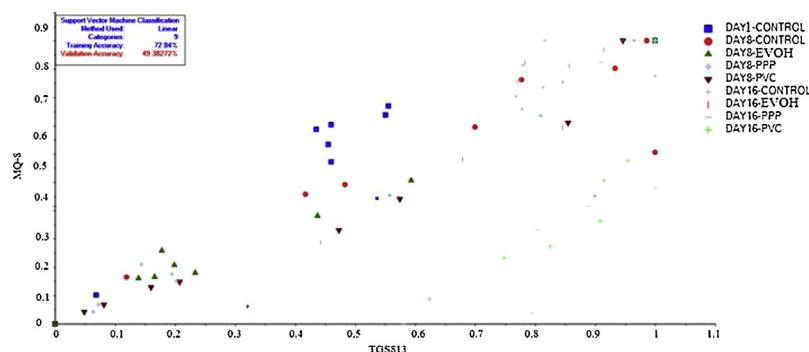


Fig. 7. SVM analysis for strawberry polymer packages on the days 1, 8 and 16 of storage for TGS813 and MQ8 sensors with linear function.

Table 4
ANOVA results for general models and prediction of sensor responses based on RSM.

Source	TGS813			MQ8		MQ4		TGS822		MQ136		MQ135		MQ3		FIS	
	df	SS	p-Value	SS	p-value	SS	p-Value	SS	p-Value	SS	p-Value	SS	p-Value	SS	p-Value	SS	p-Value
Model	5	34.78	0.00	25.47	0.00	54.01	0.00	16.24	0.00	24.30	0.00	6.93	0.00	4.64	0.00	42.68	0.00
Time	1	0.27	0.032	1.04	0.00	0.42	0.046	0.38	0.00	0.03	0.464	2×10^{-4}	0.933	0.27	0.00	1.82	0.00
Packages	1	0.21	0.057	0.20	0.01	0.3	0.093	0.10	0.134	0.04	0.381	0.062	0.154	0.037	0.00	0.14	0.297
Time × Packages	1	0.34	0.016	0.31	0.00	0.51	0.028	0.18	0.025	0.11	0.169	0.027	0.341	0.049	0.00	0.35	0.106
Time ²	1	0.36	0.014	1.13	0.00	0.54	0.24	0.43	0.00	0.06	0.302	9×10^{-4}	0.86	0.29	0.00	1.83	0.00
Packages ²	1	2.52	0.00	1.26	0.00	4.67	0.00	0.96	0.00	2.04	0.00	0.65	0.00	0.14	0.00	4.47	0.00
Residual	75	4.25		2.22		7.68		3.44		4.28		2.23		0.25		9.72	
Lack of Fit	3	1.51	0.00	0.78	0.00	2.76	0.00	0.74	0.00	1.15	0.00	0.29	0.019	0.10	0.00	1.88	0.00
Pure Error	72	2.74		1.44		4.92		2.70		3.14		7.95		0.15		7.84	
Cor Total	80	39.12		27.69		61.68		19.69		28.58		9.17		4.90		52.40	

Table 5
Summary of estimated response surface models.

Sensor	Mean	R ²	Equation
TGS813	3.30	0.8914	$Y = 1.69 + 0.91 \times \text{Time} + 1.20 \times \text{Package} - 0.122 \times \text{Time} \times \text{Package}$
MQ8	3.84	0.9197	$Y = 2.71 + 0.80 \times \text{Time} + 0.89 \times \text{Package} - 0.116 \times \text{Time} \times \text{Package}$
MQ4	3.06	0.8755	$Y = 0.904 + 1.05 \times \text{Time} + 1.64 \times \text{Package} - 0.151 \times \text{Time} \times \text{Package}$
TGS822	2.48	0.8251	$Y = 2.71 + 0.80 \times \text{Time} + 0.89 \times \text{Package} - 0.116 \times \text{Time} \times \text{Package}$
MQ136	3.13	0.8501	$Y = 1.65 + 0.65 \times \text{Time} + 1.07 \times \text{Package} - 0.069 \times \text{Time} \times \text{Package}$
MQ135	1.23	0.9164	$Y = 2 + 0.80 \times \text{Time} + 0.89 \times \text{Package} - 0.116 \times \text{Time} \times \text{Package}$
MQ3	4.62	0.9487	$Y = 4.26 + 0.384 \times \text{Time} + 0.28 \times \text{Package} - 0.046 \times \text{Time} \times \text{Package}$
FIS	3.07	0.8145	$Y = 1.05 + 0.648 \times \text{Time} + 1.66 \times \text{Package} - 0.124 \times \text{Time} \times \text{Package}$

Table 6
Best responses provided by sensors and best package by the model at the beginning of the tests.

No.	Package	TGS813	MQ8	MQ4	TGS822	MQ136	MQ135	MQ3	FIS	Desirability
1	PPP	3.949	4.279	3.873	2.866	3.733	1.602	4.795	3.595	0.901
2	PPP	3.950	4.279	3.874	2.866	3.734	1.601	4.796	3.594	0.901
3	PPP	3.948	4.278	3.872	2.866	3.733	1.604	4.795	3.596	0.901
4	EVOH	3.951	4.279	3.874	2.866	3.733	1.600	4.796	3.593	0.901
5	EVOH	3.947	4.277	3.871	2.866	3.734	1.605	4.794	3.594	0.901
6	EVOH	3.946	4.277	3.870	2.866	3.733	1.605	4.794	3.596	0.901
7	EVOH	3.952	4.279	3.875	2.864	3.731	1.591	4.797	3.584	0.900
8	EVOH	3.938	4.266	3.851	2.847	3.708	1.563	4.796	3.541	0.890
9	EVOH	3.930	4.259	3.839	2.840	3.699	1.553	4.795	3.523	0.885

Nu-SVM method, the radial basis function with an accuracy of 85.18% and 55.55%, respectively, for training and validation, had the highest classification accuracy of strawberry samples in polymer package. The results of the SVM method are shown in Table 3. Finally, the classification of strawberry samples in polymer packages on the days 1, 8 and 16 was carried out based on a linear function with an accuracy of 72.84% (Fig. 7). Qiu et al. (2015) classified strawberries with an accuracy of 25.23% using e-nose and e-tongue via SVM method.

3.4. Optimization by RSM

A summary of the results of ANOVA, and also the P-values for linear second-order, and reciprocal terms related to the second-order regression model, are presented in Table 4 for all sensors. Time variations on TGS813 and MQ4 sensor responses at the 5% significance level, and on the responses of MQ8, TGS822, MQ3, and FIS sensors were significant at the 1% level. In contrast, time variations on the response of the MQ136 and MQ135 sensors were not significant. Also, packaging affected the response of MQ8 and MQ3 sensors at the 1% levels, and for TGS813 sensor response at the 5% level. In contrast, the package treatment on the response of MQ4, TGS822, MQ136, MQ133, and FIS sensors was not significant. Considering the importance of the sensor response, after the test, the most suitable sensors were selected with the optimal responses along with the best packages at the start of the test.

We concluded that for the e-nose, MQ8, MQ3, TGS813, MQ4, and MQ136 sensors can be used to detect the strawberry headspace in EVOH, PPP, and PVC packages.

To reduce the fabrication cost, the efficiency and effectiveness of each sensor in different packages were examined using the RSM to determine which sensors are more applicable in the sample pattern recognition in different packages. MQ3, MQ8, TGS813, and MQ4 sensors had the highest ability for strawberry recognition. Using the response surface equations (Table 5), the responses of other sensors can be predicted. Among the second-order terms, there is a relationship between time and package and the response of the sensors. Among the reciprocal terms, the positive sign indicates a direct effect and the negative sign indicates the reverse relationship between variables. In the present study, all linear terms have positive sign and the interaction or second-order effect represents a negative and inverse relationship. The negative coefficients indicate that the response of the sensors is reduced by increasing the terms of interaction of time and packages.

The optimal sensor responses are shown in Table 6. Satisfaction index (desirability) indicates the strong ability and the strong relationship between sensor responses and packages. Among all the packages, the response of the sensors in the EVOH and PPP packages has the highest and most optimal values suggested by the researchers at the beginning of the test.

In Fig. 8, the contour surfaces are shown for the response of the

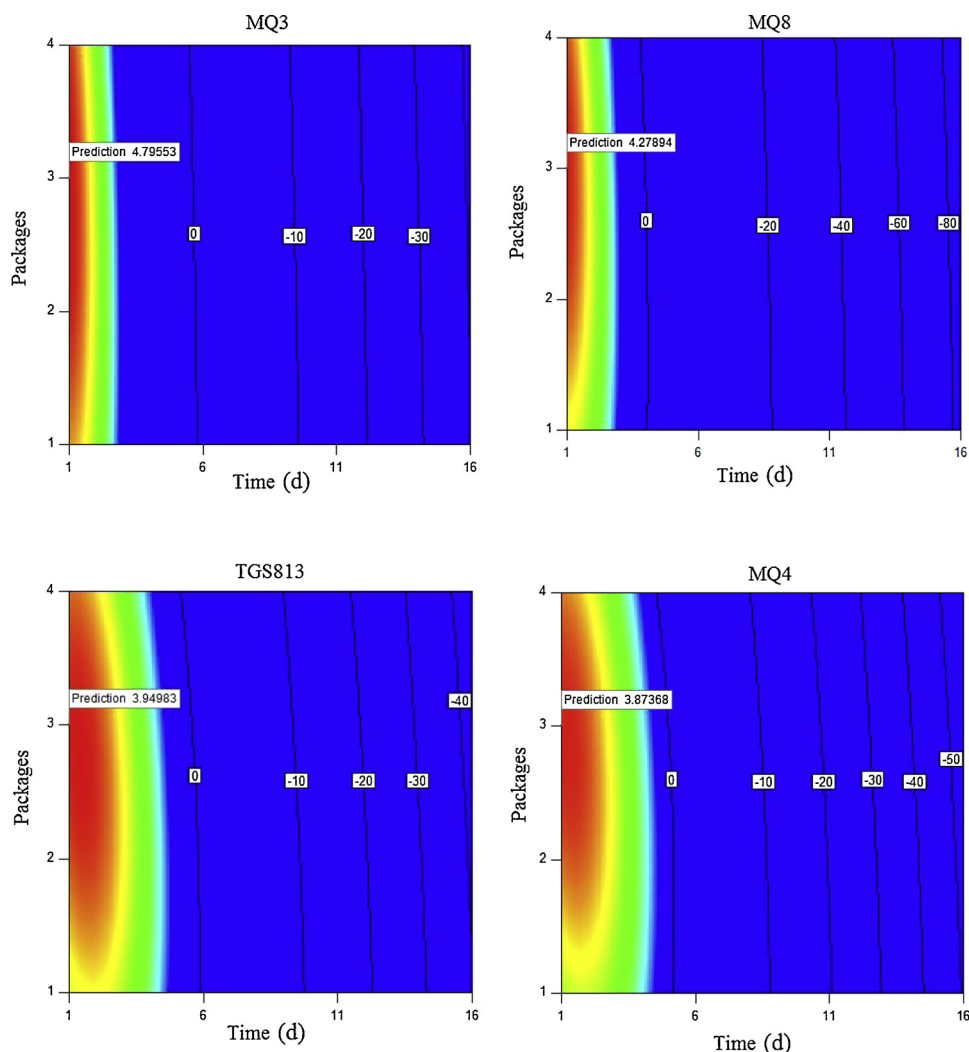


Fig. 8. Response levels contour for the best sensors selected by the model during test (1, 8 and 16 d) and 1 (control), 2 (EVOH), 3 (PPP) and 4 (PVC) packages.

sensors. The test time ranges from days 1 and 16, and the packages are encoded from 1 to 4. Based on the results, MQ3 and MQ8 sensors with the ability to detect alcohol and hydrogen were appropriate until the day 8 of storage and over time, the sensor response to the type of package has decreased, demonstrating the low stability of MQ3 in the odor recognition of strawberry samples in polymer packages. Within EVOH, PPP, and PVC packages that are resistant to moisture and ethylene, moisture and gases and oxygen, the strawberry sample presumably ripens slower due to lower respiration and removes less carbon dioxide and reduces sensor recognition relative to the early days of storage. The MQ4 and TGS813 sensors, with the ability to detect methane, propane and butane, have a higher power and stability than two previous sensors. Until day 8 of storage, the MQ4 and TGS813 sensors had the greatest ability to detect the odor of the fruit samples. These two sensors have been more applicable to both EVOH and PPP packages than the PVC package, but have low recognition ability for the control samples due to the easy removal of the gases from package.

The MQ136 and MQ135 sensors, which detect hydrogen sulfide and alcohol, ammonia, benzene, and carbon dioxide, respectively, had good detection capability for all packages. The MQ135 sensor has the highest detection capability in packages because these packages do not allow carbon dioxide diffusion, and accumulation of the gas would presumably slow fruit ripening. So this type of sensor can also be used. The TGS822 sensor is capable of detecting organic solvent vapor and in these packages. Owing to the low detection limit, FIS was not able to

detect the headspace of strawberry samples (Fig. 9).

4. Conclusion

The application of polymer packages on strawberry fruit was investigated using an e-nose system based on an eight metal oxide semiconductor sensors array in combination with pattern recognition methods such as PCA, LDA and SVM. Fruit freshness were well classified with unpackaged and packaged samples using pattern recognition methods. The PCA method explained 84% of the total variance of data. The LDA method categorized all sensor response data with high accuracy. On the other hand, SVM in Nu-SVM and C-SVM resulted in the highest classification accuracy by radial and polynomial basis function, respectively. The sensors were identified using an optimization method with response surface to detect the headspace pattern of the strawberry samples. According to the results, MQ8, MQ3, MQ135, MQ136, MQ4, and TGS813 sensors were selected as the best sensors for use in an e-nose system.

Acknowledgement

This work has been financially supported by the research deputy of Shahrekord University. The grant number was 141.679.

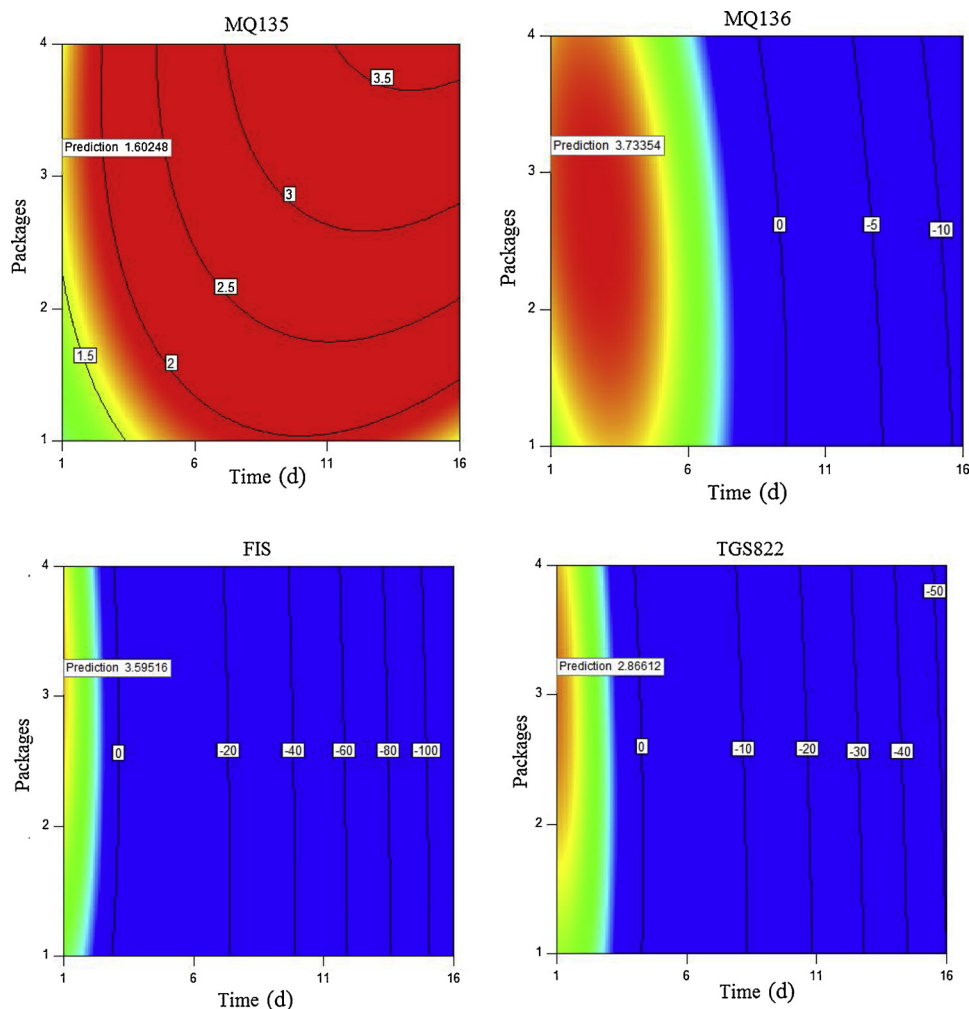


Fig. 9. Response levels contour for the best sensors selected by the model during test (1, 8 and 16 d) and 1 (control), 2 (EVOH), 3 (PPP) and 4 (PVC) packages.

References

- Ait-Sahalia, Y., Xiu, D., 2018. Principal component analysis of high-frequency data. *J. Am. Stat. Assoc.* 1–17. <https://doi.org/10.1080/01621459.2017.1401542>.
- Baskar, C., Nesakumar, N., Rayappan, J.B.B., Doraipandian, M., 2017. A framework for analysing E-nose data based on fuzzy set multiple linear regression: paddy quality assessment. *Sens. Actuators A: Phys.* 267, 200–209. <https://doi.org/10.1016/j.sna.2017.10.020>.
- Emamifar, A., Kadivar, M., Shahedi, M., Soleimani-Zad, S., 2011. Effect of nano-composite packaging containing Ag and ZnO on inactivation of *Lactobacillus plantarum* in orange juice. *Food Control* 22 (3–4), 408–413. <https://doi.org/10.1016/j.foodcont.2010.09.011>.
- Esteki, M., Farajmand, B., Kolahderazi, Y., Simal-Gandara, J., 2017. Chromatographic fingerprinting with multivariate data analysis for detection and quantification of apricot kernel in almond powder. *Food Anal. Methods* 10, 3312–3320. <https://doi.org/10.1007/s12161-017-0903-5>.
- Gadhiya, D., Shah, N.P., Patel, A.R., Prajapati, J.B., 2018. Preparation and shelf life study of probiotic chocolate manufactured using *Lactobacillus helveticus* MTCC 5463. *Acta Alimentaria* 47 (3), 350–358. <https://doi.org/10.1556/066.2018.47.3.11>.
- Ghasemi-Varnamkhasti, M., Mohtasebi, S.S., Siadat, M., Lozano, J., Ahmadi, H., Razavi, S.H., Dicko, A., 2011. Aging fingerprint characterization of beer using electronic nose. *Sens. and Actuators B: Chem.* 159, 51–59. <https://doi.org/10.1016/j.snb.2011.06.036>.
- Ghasemi-Varnamkhasti, M., Mohtasebi, S.S., Siadat, M., Ahmadi, H., Razavi, S.H., 2015. From simple classification methods to machine learning for the binary discrimination of beers using electronic nose data. *Eng. Agric. J. Food Agric. Environ.* 8, 44–51. <https://doi.org/10.1016/j.eaef.2014.07.002>.
- Ghasemi-Varnamkhasti, M., Mohammad-Razdari, A., Yoosefian, S.H., Izadi, Z., 2018a. Effect of the combination of gamma irradiation and Ag nanoparticles polyethylene films on the quality of fresh bottom mushroom (*Agaricus bisporus* L.). *J. Food Process. Preserv.*, e13652. <https://doi.org/10.1111/jfpp.13652>.
- Ghasemi-Varnamkhasti, M., Tohidi, M., Mishra, P., Izadi, Z., 2018b. Temperature modulation of electronic nose combined with multi-class support vector machine classification for identifying export caraway cultivars. *Postharvest Biol. Technol.* 138, 134–139. <https://doi.org/10.1016/j.postharvbio.2018.01.011>.
- Haddi, Z., Alami, H., ElBari, N., Tounsi, M., Barhoumi, H., Maaref, A., Jaffrezic-Renault, N., Bouchikhi, B., 2013. Electronic nose and tongue combination for improved classification of Moroccan virgin olive oil profiles. *Food Res. Int.* 54, 1488–1498. <https://doi.org/10.1016/j.foodres.2013.09.036>.
- Jolayemi, O.S., Tokatli, F., Buratti, S., Alamprese, C., 2017. Discriminative capacities of infrared spectroscopy and e-nose on Turkish olive oils. *Eur. Food Res. Technol.* 243 (11), 2035–2042. <https://doi.org/10.1007/s00217-017-2909-z>.
- Karami, H.R., Keyhani, M., Mowla, D., 2016. Experimental analysis of drag reduction in the pipelines with response surface methodology. *J. Petrol. Sci. Eng.* 138, 104–112. <https://doi.org/10.1016/j.petrol.2015.11.041>.
- Kiani, S., Minaei, S., Ghasemi-Varnamkhasti, M., 2017. Integration of computer vision and electronic nose as non-destructive systems for saffron adulteration detection. *Comput. Electron. Agric.* 141, 46–53. <https://doi.org/10.1016/j.compag.2017.06.018>.
- Kiani, S., Minaei, S., Ghasemi-Varnamkhasti, M., 2018. Real-time aroma monitoring of mint (*Mentha spicata* L.) leaves during the drying process using electronic nose system. *Measurement* 124, 447–452. <https://doi.org/10.1016/j.measurement.2018.03.033>.
- Lin, Y.P., Lee, T.Y., Tsen, J.H., King, V.A.E., 2007. Dehydration of yam slices using FIR-assisted freeze drying. *J. Food Eng.* 79 (4), 1295–1301. <https://doi.org/10.1016/j.jfoodeng.2006.04.018>.
- Liu, F., Tang, X., 2017. Investigation on strawberry freshness by rapid determination using an artificial olfactory system. *Int. J. Food Prop.* 20 (sup1), S910–S920. <https://doi.org/10.1080/10942912.2017.1315595>.
- Men, H., Shi, Y., Jiao, Y., Gong, F., Liu, J., 2018. Electronic nose sensors data feature mining: a synergetic strategy for the classification of beer. *Anal. Methods* 10, 2016–2025. <https://doi.org/10.3390/s19020419>.
- Moon, H.G., Jung, Y., Han, S.D., Shim, Y.S., Jung, W.S., Lee, T., Park, H.H., 2018. All villi-like metal oxide nanostructures-based chemiresistive electronic nose for an exhaled breath analyzer. *Sens. Actuators B: Chem.* 257, 295–302. <https://doi.org/10.1016/j.snb.2017.10.153>.
- Moradi, S., Chow, C.W., Van Leeuwen, J., Cook, D., Drikas, M., Hayde, P., Amal, R., 2018. Optimization of operational water quality parameters in a drinking water distribution system using response surface methodology. *World Academy of Science, Engineering and Technology. Int. J. Environ. Ecol. Eng.* 5 (5). <https://doi.org/10.1007/s13197->

- 014-1431-6.
- Ordukaya, E., Karlik, B., 2017. Quality control of olive oils using machine learning and electronic nose. *J. Food Qual.* <https://doi.org/10.1155/2017/9272404>.
- Pan, L., Zhang, W., Zhu, N., Mao, S., Tu, K., 2014. Early detection and classification of pathogenic fungal disease in post-harvest strawberry fruit by electronic nose and gas chromatography–mass spectrometry. *Food Res. Int.* 62, 162–168. <https://doi.org/10.1016/j.foodres.2014.02.020>.
- Qiu, S., Wang, J., Gao, L., 2014. Discrimination and characterization of strawberry juice based on electronic nose and tongue: comparison of different juice processing approaches by LDA, PLSR, RF, and SVM. *J. Agric. Food Chem.* 62 (27), 6426–6434. <https://doi.org/10.1021/jf501468b>.
- Qiu, S., Gao, L., Wang, J., 2015. Classification and regression of ELM, LVQ and SVM for E-nose data of strawberry juice. *J. Food Eng.* 144, 77–85. <https://doi.org/10.1016/j.jfoodeng.2014.07.015>.
- Sanaeifar, A., Mohtasebi, S.S., Ghasemi-Varnamkhasti, M., Ahmadi, H., 2016. Application of MOS based electronic nose for the prediction of banana quality properties. *Measurement* 82, 105–114. <https://doi.org/10.1016/j.measurement.2015.12.041>.
- Silva, I.A., Souza, A.M., Bromley, T.R., Cianciaruso, M., Marx, R., Sarthour, R.S., Adesso, G., 2016. Observation of time-invariant coherence in a nuclear magnetic resonance quantum simulator. *Phys. Rev. Lett.* 117 (16), 160402. <https://doi.org/10.1103/PhysRevLett.117.160402>.
- Tahri, K., Tiebe, C., El Bari, N., Hübert, T., Bouchikhi, B., 2017. Geographical classification and adulteration detection of cumin by using electronic sensing coupled to multivariate analysis. *J. Mater. Process. Technol.* 27, 240–241. <https://doi.org/10.1016/j.protcy.2017.04.102>.
- Tharwat, A., Gaber, T., Ibrahim, A., Hassanien, A.E., 2017. Linear discriminant analysis: a detailed tutorial. *AI Communications* 30 (2), 169–190. <https://doi.org/10.3233/AIC-170729>.
- Tohidi, M., Ghasemi-Varnamkhasti, M., Ghafarina, V., Mohtasebi, S.S., Bonyadian, M., 2018. Identification of trace amounts of detergent powder in raw milk using a customized low-cost artificial olfactory system: a novel method. *Measurement* 124, 120–129. <https://doi.org/10.1016/j.measurement.2018.04.006>.
- Varmuza, K., Filzmoser, P., 2009. *Introduction to Multivariate Statistical Analysis in Chemometrics*. CRC Press, Boca Raton. <https://doi.org/10.1201/9781420059496>.
- Zhou, Y., Peng, J., Chen, C.P., 2015. Extreme learning machine with composite kernels for hyperspectral image classification. *IEEE J. Sel. Top. Appl. Earth Obs. Remote Sens.* 8 (6), 2351–2360. <https://doi.org/10.1109/JSTARS.2014.2359965>.